ISSN 0016-7037
Volume 74, Number 14
July 15, 2010

Geochimica et Cosmochimica Acta

JOURNAL OF THE GEOCHEMICAL SOCIETY
AND THE METEORITICAL SOCIETY

Volume 74, Number 14 July 15, 2010

Articles

Continued on outside back cover

Available online at www.sciencedirect.com
ScienceDirect
Geochimica et Cosmochimica Acta 74 (2010) 4150–4166
Geochimica et Cosmochimica Acta
www.elsevier.com/locate/gca

Magnesium isotopic composition of the Earth and chondrites

Fang-Zhen Teng [a,*], Wang-Ye Li [a,b], Shan Ke [a,c], Bernard Marty [d], Nicolas Dauphas [e], Shichun Huang [f], Fu-Yuan Wu [g], Ali Pourmand [h]

[a] *Isotope Laboratory, Department of Geosciences & Arkansas Center for Space and Planetary Science, University of Arkansas, Fayetteville, AR 72701, USA*
[b] *CAS Key Laboratory of Crust–Mantle Materials and Environments, School of Earth and Space Sciences, University of Science and Technology of China, Hefei 230026, China*
[c] *State Key Laboratory of Geological Processes and Mineral Resources, School of Earth Science and Mineral Resources, China University of Geosciences, Beijing 100083, China*
[d] *Centre de Recherches Pétrographiques et Géochimiques, CNRS, 15 rue Notre-Dame-des-Pauvres, 54501 Vandoeuvre-lès-Nancy, France*
[e] *Origins Laboratory, Department of the Geophysical Sciences and Enrico Fermi Institute, The University of Chicago, 5734 South Ellis Ave., Chicago, IL 60637, USA*
[f] *Department of Earth and Planetary Sciences, Harvard University, 20 Oxford Street, Cambridge, MA 02138, USA*
[g] *State Key Laboratory of Lithospheric Evolution, Institute of Geology and Geophysics, Chinese Academy of Sciences, Beijing 100029, China*
[h] *Department of Marine Geology and Geophysics, University of Miami, 4600 Rickenbacker Causeway, Miami, FL 33149, USA*

Received 4 December 2009; accepted in revised form 19 April 2010; available online 27 April 2010

Abstract

To constrain further the Mg isotopic composition of the Earth and chondrites, and investigate the behavior of Mg isotopes during planetary formation and magmatic processes, we report high-precision ($\pm 0.06‰$ on $\delta^{25}Mg$ and $\pm 0.07‰$ on $\delta^{26}Mg$, 2SD) analyses of Mg isotopes for (1) 47 mid-ocean ridge basalts covering global major ridge segments and spanning a broad range in latitudes, geochemical and radiogenic isotopic compositions; (2) 63 ocean island basalts from Hawaii (Kilauea, Koolau and Loihi) and French Polynesia (Society Island and Cook-Austral chain); (3) 29 peridotite xenoliths from Australia, China, France, Tanzania and USA; and (4) 38 carbonaceous, ordinary and enstatite chondrites including 9 chondrite groups (CI, CM, CO, CV, L, LL, H, EH and EL).

Oceanic basalts and peridotite xenoliths have similar Mg isotopic compositions, with average values of $\delta^{25}Mg = -0.13 \pm 0.05$ (2SD) and $\delta^{26}Mg = -0.26 \pm 0.07$ (2SD) for global oceanic basalts ($n = 110$) and $\delta^{25}Mg = -0.13 \pm 0.03$ (2SD) and $\delta^{26}Mg = -0.25 \pm 0.04$ (2SD) for global peridotite xenoliths ($n = 29$). The identical Mg isotopic compositions in oceanic basalts and peridotites suggest that equilibrium Mg isotope fractionation during partial melting of peridotite mantle and magmatic differentiation of basaltic magma is negligible. Thirty-eight chondrites have indistinguishable Mg isotopic compositions, with $\delta^{25}Mg = -0.15 \pm 0.04$ (2SD) and $\delta^{26}Mg = -0.28 \pm 0.06$ (2SD). The constancy of Mg isotopic compositions in all major types of chondrites suggest that primary and secondary processes that affected the chemical and oxygen isotopic compositions of chondrites did not significantly fractionate Mg isotopes.

Collectively, the Mg isotopic composition of the Earth's mantle, based on oceanic basalts and peridotites, is estimated to be -0.13 ± 0.04 for $\delta^{25}Mg$ and -0.25 ± 0.07 for $\delta^{26}Mg$ (2SD, $n = 139$). The Mg isotopic composition of the Earth, as represented by the mantle, is similar to chondrites. The chondritic composition of the Earth implies that Mg isotopes were well mixed during accretion of the inner solar system.

* Corresponding author. Tel.: +1 4795754524; fax: +1 4795753469.
E-mail address: fteng@uark.edu (F.-Z. Teng).

0016-7037/$ - see front matter © 2010 Elsevier Ltd. All rights reserved.
doi:10.1016/j.gca.2010.04.019

1. INTRODUCTION

Studies of the Mg isotopic composition of the Earth are important for understanding its geochemistry and may shed light on the accretion history of the Earth (Norman et al., 2006; Wiechert and Halliday, 2007). However, the Mg isotopic composition of the Earth has remained poorly constrained, and is highly debated. There is uncertainty in the magnitude of Mg isotope fractionation at mantle temperatures (Young and Galy, 2004; Pearson et al., 2006; Handler et al., 2009; Yang et al., 2009; Young et al., 2009) and whether the Earth has a chondritic Mg isotopic composition or not (Teng et al., 2007; Wiechert and Halliday, 2007; Chakrabarti and Jacobsen, 2009; Handler et al., 2009; Yang et al., 2009; Young et al., 2009; Dauphas et al., 2010). These uncertainties mainly result from the limited database for terrestrial samples and meteorites, as well as possible analytical artifacts in high-precision Mg isotopic analysis by multi-collector inductively coupled plasma mass spectrometer (MC-ICPMS).

Knowledge about the composition of the mantle is derived largely from studies of peridotite xenoliths (Jagoutz et al., 1979; McDonough and Sun, 1995), and oceanic basalts, which are products of decompression melting of the mantle (Hofmann, 2003). In order to use oceanic basalts to precisely constrain isotopic compositions of their mantle sources, it requires that isotope fractionation is absent during partial melting and basalt differentiation. Teng et al. (2007) investigated a set of well-characterized samples from Kilauea Iki lava lake, ranging from olivine-rich picrites to low-MgO andesites, and found no measurable Mg isotope fractionation resulting from basalt differentiation, suggesting that oceanic basalts can be used to study the Mg isotopic composition of the mantle.

Here, we analyzed Mg isotopes for ~200 mantle-related rocks and chondrites in order to further constrain the Mg isotopic composition of the terrestrial mantle and chondrites, and investigate Mg isotope fractionation during planetary formation and magmatic processes. These samples encompass mid-ocean ridge basalts (MORBs), ocean island basalts (OIBs), peridotite xenoliths, and all major types of chondrites. The large database thus allows comparisons of Mg isotopic compositions between these different types of materials without bias resulting from inter-laboratory comparisons. Our results show that, at the current level of precision and accuracy (±0.06‰ on δ^{25}Mg and ±0.07‰ on δ^{26}Mg, see Table 1 for definitions of δ^{25}Mg and δ^{26}Mg), equilibrium Mg isotope fractionation during partial melting of peridotite and crystal fractionation of basaltic magma is negligible. The bulk Earth, as represented by global oceanic basalts and peridotites, has a chondritic Mg isotopic composition.

2. SAMPLES

A globally dispersed, geochemically diverse set of well-characterized fresh samples, including 47 MORBs covering global major ridge segments, 63 OIBs from Hawaiian and French Polynesian islands, 29 peridotite xenoliths from Australia, China, France, Tanzania and USA, and 38 chondrites covering the whole spectrum of chondrites have been investigated (Fig. 1). The petrology, mineralogy, chemical and isotopic composition of these samples have been presented in previous publications (Jagoutz et al., 1979; Helz, 1987; McDonough and McCulloch, 1987; Jochum et al., 1989; Dewey et al., 1990; Chauvel et al., 1992; Rudnick et al., 1993, 1994; Woodhead et al., 1993; Marty and Humbert, 1997; Lassiter and Hauri, 1998; Marty and Tolstikhin, 1998; Chesley et al., 1999; Lee and Rudnick, 1999; Marty and Zimmermann, 1999; Marty and Dauphas, 2003; Huang and Frey, 2005; Wu et al., 2006). Nevertheless, a brief description is given below.

2.1. MORBs

MORB samples investigated here are from zero-aged centered ridge sections including the Mid-Atlantic Ridge at 30–36°N, the East Pacific Rise at 06°N, 13°N, 17–19°S, and 21°N, the Indian Ridge system near the Rodriguez Triple Junction and at 39°S, and the Red Sea at 18°N and 20°N. In addition, samples from the North Fiji Basin, the world's largest back-arc basin, have also been analyzed.

Our studied basalts cover most major mid-oceanic ridge segments, are well-characterized and span a broad range in latitudes, geochemical and isotopic compositions. They vary from normal MORB (N-MORB), transitional MORB (T-MORB) to enriched MORB (E-MORB). Their major element compositions range from 6.4 to 9.7 wt% in MgO, from 0.03 to 0.31 wt% in K_2O, from 0.76 to 2.27 wt% in TiO_2 and from 0.02 to 0.21 in K_2O/TiO_2 ratios. The spreading rates vary from 1–2 cm/year for the Mid-Atlantic Ridge to 8–9 cm/year for the East Pacific Rise (Marty and Humbert, 1997; Marty and Tolstikhin, 1998; Marty and Zimmermann, 1999).

2.2. OIBs

The OIBs are mainly from two well-studied groups of islands in the Pacific Ocean: Hawaiian volcanoes (Koolau, Loihi and Kilauea) and French Polynesia islands (Society Island and Cook-Austral chain).

Twenty-two tholeiitic samples from Koolau Volcano, Hawaii have been measured here (e.g., Frey et al., 1994; Roden et al., 1994; Norman and Garcia, 1999; Haskins and Garcia, 2004; Huang and Frey, 2005; Salters et al., 2006). In addition, two alkaline basalt samples from Loihi Seamount were also investigated. Loihi Seamount is the youngest volcanic center growing from the seabed about 35 km southeast of the Hawaii Island and is in the pre-shield state (Moore et al., 1982; Garcia et al., 1993, 1995; Valbracht et al., 1996). Finally, 14 samples from Kilauea Iki lava lake, most of which have been analyzed before at the Field Museum (Teng et al., 2007), were re-analyzed here to eliminate potential inter-laboratory discrepancies.

The 25 samples from French Polynesia islands investigated here are mainly from the Society Island and Cook-Austral chain. They are enriched in incompatible trace elements and radiogenic isotopes, and are highly variable in nitrogen isotopic compositions. These geochemical and isotopic features have been interpreted to result from mixing of up

Table 1
Magnesium isotopic compositions of seawater, Cambridge-1, olivine, rock and synthetic standards.

Standard	Type	δ^{25}Mg	2SD	δ^{26}Mg	2SD
IL-Mg-1	Synthetic	0.00	0.06	0.01	0.07
Replicate		0.01	0.06	0.03	0.07
Replicate		0.04	0.06	0.05	0.01
Replicate		0.05	0.06	0.04	0.06
Replicate		−0.01	0.06	−0.02	0.09
Replicate		−0.01	0.06	−0.00	0.05
Replicate		−0.05	0.06	−0.01	0.08
Replicate		0.01	0.06	−0.01	0.08
Replicate		−0.04	0.06	−0.03	0.08
Replicate		−0.04	0.05	−0.07	0.10
Replicate		−0.04	0.04	−0.04	0.07
Replicate		−0.03	0.03	−0.04	0.07
Replicate		−0.00	0.05	−0.01	0.07
Average		−0.01	0.06	−0.01	0.07
Hawaii SW	Seawater	−0.43	0.08	−0.79	0.06
Replicate		−0.45	0.02	−0.86	0.05
Replicate		−0.42	0.05	−0.81	0.07
Replicate		−0.42	0.05	−0.84	0.04
Average		−0.43	0.03	−0.83	0.06
Cambridge-1	Pure Mg	−1.36	0.06	−2.65	0.09
Replicate		−1.35	0.05	−2.61	0.08
Average		−1.36	0.01	−2.63	0.06
KH	Olivine	−0.15	0.07	−0.27	0.10
Replicate		−0.16	0.15	−0.36	0.10
Replicate		−0.16	0.07	−0.31	0.10
Replicate		−0.19	0.05	−0.32	0.10
Replicate		−0.14	0.06	−0.26	0.09
Replicate		−0.14	0.06	−0.27	0.06
Replicate		−0.14	0.06	−0.26	0.08
Replicate		−0.14	0.05	−0.26	0.06
Replicate		−0.13	0.05	−0.23	0.06
Replicate		−0.12	0.05	−0.24	0.07
Replicate		−0.17	0.03	−0.29	0.04
Replicate		−0.13	0.06	−0.24	0.08
Replicate		−0.13	0.06	−0.24	0.08
Replicate		−0.11	0.06	−0.23	0.08
Replicate		−0.13	0.06	−0.24	0.08
Replicate		−0.13	0.04	−0.28	0.06
Average		−0.14	0.04	−0.27	0.07
DTS-2	Dunite, OB	−0.13	0.07	−0.27	0.10
Replicate		−0.15	0.06	−0.30	0.09
Replicate		−0.16	0.05	−0.30	0.10
Replicate		−0.16	0.06	−0.33	0.05
Replicate		−0.18	0.04	−0.34	0.06
Replicate		−0.18	0.05	−0.32	0.07
DTS-2	Bomb	−0.14	0.05	−0.29	0.06
Average		−0.16	0.04	−0.31	0.05
Allende	Chondrite, OB	−0.10	0.12	−0.28	0.01
Allende	Bomb	−0.17	0.07	−0.28	0.10
Replicate		−0.17	0.06	−0.34	0.09
Replicate		−0.16	0.06	−0.32	0.08
Replicate		−0.15	0.04	−0.29	0.06
Replicate		−0.16	0.04	−0.31	0.05
Replicate		−0.17	0.04	−0.32	0.06
Allende	Flux	−0.16	0.05	−0.28	0.09
Allende	Flux	−0.15	0.05	−0.27	0.09
Average		−0.15	0.04	−0.30	0.05
Murchison	Chondrite, OB	−0.17	0.06	−0.31	0.06
Murchison	Bomb	−0.14	0.06	−0.26	0.06
Replicate		−0.18	0.06	−0.34	0.07
Replicate		−0.17	0.05	−0.33	0.08
Average		−0.17	0.03	−0.31	0.07
SUNY	MORB	−0.13	0.05	−0.23	0.06

$\delta^{x}Mg = [(^{x}Mg/^{24}Mg)_{sample}/(^{x}Mg/^{24}Mg)_{DSM3} - 1] \times 1000$, where $x = 25$ or 26 and DSM3 is Mg solution made from pure Mg metal (Galy et al., 2003). 2SD = 2 times the standard deviation of the population of 4 repeat measurements of a sample solution. IL-Mg-1 is a synthetic solution with concentration ratios of Mg:Fe:Al:Ca:Na:K:Ti = 1:1:1:1:1:1:0.1. Replicate refers to repeat column chemistry and measurement of different aliquots of a stock solution. Bomb refers to sample dissolution by high-pressure bomb. Flux refers to sample dissolution by lithium-metaborate flux (Pourmand and Dauphas, 2010). OB refers to open-beaker dissolution. See text for details.

to 9% recycled crust with a substantial proportion of pelagic sediments (Dewey et al., 1990; Chauvel et al., 1992; Woodhead et al., 1993; Marty and Dauphas, 2003).

2.3. Peridotite xenoliths

The 29 peridotite samples investigated here are from nine different localities on five continents (Fig. 1) and include lherzolite, harzburgite and dunite as well as wehrlite and glimmerite. They have experienced various degrees of early melt extraction and later metasomatism, and have been used to study the composition and evolution of the lithospheric mantle (Frey and Green, 1974; Jagoutz et al., 1979; McDonough and McCulloch, 1987; Jochum et al., 1989; Rudnick et al., 1993, 1994; Handler et al., 1997; Chesley et al., 1999; Lee and Rudnick, 1999; Wu et al., 2006).

The three fertile spinel lherzolite samples from USA and France (KH-1, Kilbourne Hole, New Mexico, USA; Po-1, Potrillo, New Mexico, USA and Fr-1, Landoz, Massif Central, France) were previously used to estimate major and trace element distributions in the upper mantle (Jagoutz et al., 1979; Jochum et al., 1989). Two Proterozoic fertile spinel lherzolites from southeast Australia were analyzed to study the composition of the southeast Australian lithospheric mantle (Frey and Green, 1974; McDonough and McCulloch, 1987; Handler et al., 1997).

In addition to these fertile spinel lherzolite samples, two sets of well-characterized peridotite xenoliths, including lherzolite, harzburgite, dunite, wehrlite and glimmerite from North China and Northern Tanzania, were also analyzed (Rudnick et al., 1993, 1994; Chesley et al., 1999; Lee and Rudnick, 1999; Wu et al., 2006). These samples have experienced various types of metasomatism and different degrees of partial melting, and are therefore well suited for Mg isotopic analysis to evaluate these effects.

Peridotite samples from North China were collected from alkaline basalts from the Huangyishan volcano,

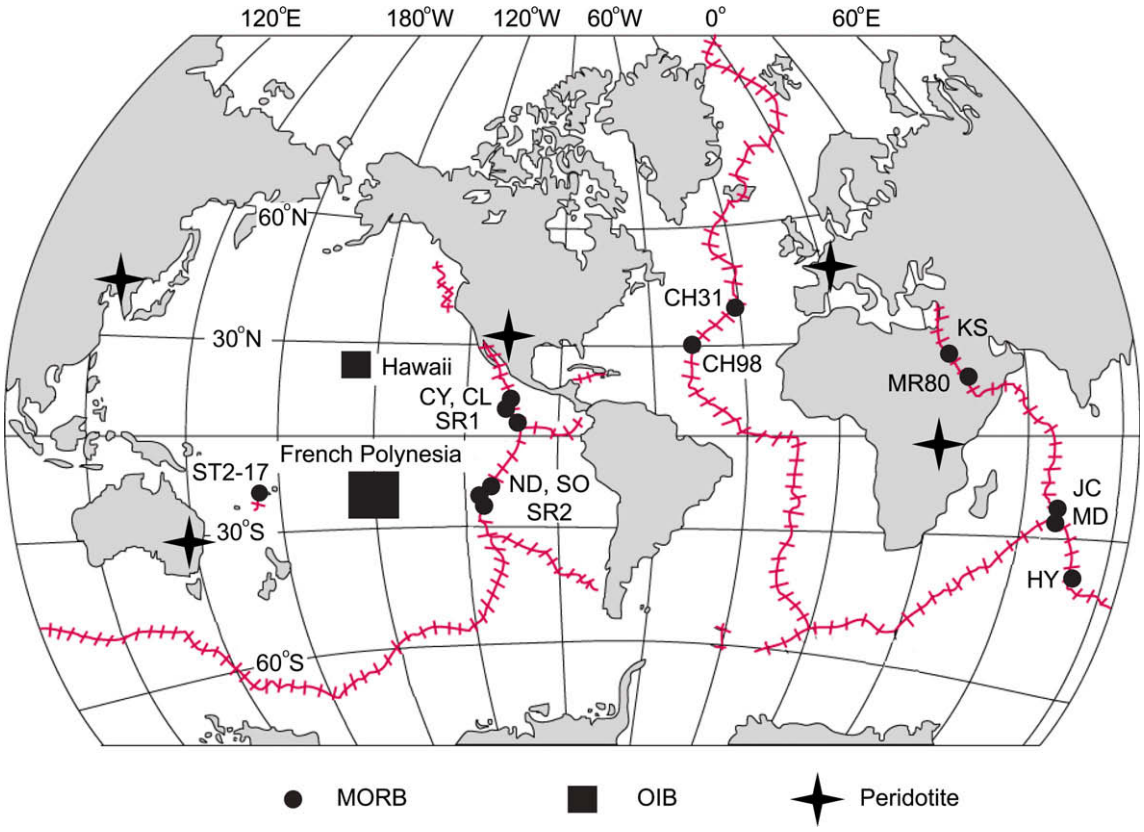

Fig. 1. Sample location map for mid-ocean ridge basalts (MORBs), ocean island basalts (OIBs) and peridotite xenoliths investigated in this study.

Kuandian (Wu et al., 2006). Kuandian peridotites are ~2.3 Ga old, range from refractory harzburgite to relatively fertile lherzolite and have undergone various degrees of metasomatic alteration. Sample HY2-06 contains approximately 2% amphibole, indicating modification via aqueous fluid and/or melt metasomatism (Wu et al., 2006).

Samples from Northern Tanzania were collected from three Quaternary rift-related volcanoes: the Lashaine tuff cone, the Olmani cinder cone and the Labait tuff cone (Rudnick et al., 1993, 1994; Chesley et al., 1999; Lee and Rudnick, 1999). They are dated at 2.5–2.9 Ga (Chesley et al., 1999). Lashaine peridotites range from refractory garnet harzburgite through fertile garnet lherzolite to metasomatised dunite. Olmani peridotites have experienced different degrees of carbonatite metasomatism and range from refractory garnet harzburgite to clinopyroxene-bearing, orthopyroxene-free dunite and wehrlite (Rudnick et al., 1993). The Labait garnet lherzolite (LB-45) is derived from near the lithosphere–asthenosphere boundary and has a major element composition similar to the primitive upper mantle (Lee and Rudnick, 1999). The Labait glimmerite (LB-49) is a metasomatic end member that represents metasomatic melt from the East African Rift (Chesley et al., 1999).

2.4. Chondrites

Chondrites possess various unique chemical and physical features that make them particularly useful tracers of the origin and evolution of the early solar system (e.g., Scott and Krot, 2003). They provide the best estimate of solar system abundances for non-volatile elements and are considered to represent the essential building blocks of terrestrial planets.

The majority of 38 chondrites analyzed here were falls. They represent all three major chondrite classes (carbonaceous, ordinary and enstatite), from 9 chondrite groups (CI, CM, CO, CV, L, LL, H, EH and EL), vary from 1 to 7 in petrologic grade and cover the whole range of calcium–aluminum-rich inclusion (CAI) content (from <0.01 vol % in CI chondrites up to ~13 vol % in CO chondrites), chemical and isotopic composition, and oxidation states found in undifferentiated meteorites (e.g., Scott and Krot, 2003).

3. ANALYTICAL METHODS

Magnesium isotopic analysis was carried out at the Isotope Laboratory of the University of Arkansas, Fayetteville. Procedures for sample dissolution, column chemistry and instrumental analysis are similar to those reported in previous studies (Teng et al., 2007; Yang et al., 2009) and only a brief description is given below.

3.1. Sample preparation and chromatography

Whole-rock basalts and olivine grains came from aliquots of solutions used in a previous Fe isotope study (Teng

et al., 2008). All chondrites (80–105 mg homogenized powder) except Murchison were fused with Puratonic® lithium-metaborate ($LiBO_2$) flux in 8 mL ultra-pure graphite crucibles at 1070 °C for 12 min at the Origins Laboratory of the University of Chicago. This flux-fusion procedure ensured that even the most chemically-resistant phases found in meteorites (e.g., SiC) were digested. The fusion melt was directly dissolved in 3 N HNO_3 and loaded onto 2 mL TODGA resin in extraction chromatography cartridges stationed on a vacuum chamber. Calcium and rare-earth elements (REEs) were removed from the solution using the method described in Pourmand and Dauphas (2010). For comparison, Murchison and some of Allende chondrites were also digested by prolonged acid dissolution in Parr bombs and open-beaker dissolution. All peridotites (~0.5–1 mg) were dissolved by using a combination of HF–HNO_3–HCl in the Isotope Laboratory at the University of Arkansas, following established methods (Teng et al., 2007; Yang et al., 2009). No spinel residue was observed under microscope in the solution. In preparation for chromatographic separation, all sample solutions were evaporated to dryness, fluxed with concentrated HNO_3, and finally dissolved in 1 N HNO_3.

Separation of Mg was achieved by cation exchange chromatography with Bio-Rad 200–400 mesh AG50W-X8 pre-cleaned resin in 1 N HNO_3 by following the similar procedure described by Teng et al. (2007). Briefly, samples containing ~10 μg of Mg were loaded on the resin and eluted with 1 N HNO_3. At least 2 standards (synthetic solution, olivine standard, peridotite standard or chondrite sample) were processed with 8 unknown samples for each batch of column chemistry. The column chromatography step was repeated to separate Mg from Na, Al, K, Ca and Fe and obtain a pure Mg solution. An additional anion exchange chromatography step with Bio-Rad 200–400 mesh AG1-X8 pre-cleaned resin in 1 N HCl–0.5 N HF was applied to some of chondrite samples to separate Mg from Ti. Procedure blank was <10 ng, which represented <0.1% of Mg loaded on the column. This chromatographic procedure, however, does not quantitatively separate Ni from Mg. Doping experiments show that under "wet" plasma conditions, no significant deviation of δ^{26}Mg is observed within our external precision (~0.07‰), even when the Ni/Mg concentration ratio reaches 2 (Fig. 2). Although the effect of Ni can be dramatic for Ni-rich and Mg-poor samples (e.g., spinels) analyzed by "dry" plasma (Fig. 2), the Ni/Mg ratios in all samples were <0.3. Consequently, the presence of Ni did not affect the accuracy of Mg isotopic measurements.

3.2. Mass spectrometry

Magnesium isotopic compositions were analyzed by the sample-standard bracketing method on a *Nu Plasma* HR-MC-ICPMS at the Isotope Laboratory of the University of Arkansas.

Two introduction systems were utilized for the analysis of purified Mg sample solution (~200 ppb Mg in ~0.45 N HNO_3 solution). A quartz cyclonic spray chamber (Elemental Scientific Inc.) and a MicroMist micro-uptake glass concentric nebulizer (Glass Expansion) were used for "wet" plasma. Alternatively, a DSN-100 desolvation nebulizer system (Nu Instruments) was used for "dry" plasma conditions. Magnesium isotopes were analyzed in a low-resolution mode, with ^{26}Mg, ^{25}Mg and ^{24}Mg measured simultaneously in separate Faraday cups (H5, Ax and L4). Higher precision was achieved on ^{26}Mg/^{24}Mg and ^{25}Mg/^{24}Mg ratios with "wet" plasma. Loss in sensitivity (30 V/200 ppb Mg vs. 4 V/200 ppb Mg with an uptake rate of 100 μl/min) was largely compensated by a significant gain in stability, similar to Fe isotopes measured by sample-standard bracketing methods (Dauphas et al., 2009b). Therefore, during the course of this study, "wet" plasma was used for all sample analyses. The background Mg signals for ^{24}Mg were always $<10^{-4}$ V and were negligible relative to sample signals (3–4 V) given our external precision of ~0.07‰.

3.3. Precision and accuracy

Precision and accuracy of the analyses were assessed by conducting full procedural replicates of synthetic solutions, seawater, rocks, minerals and pure Mg standards. The in-run precision on the ^{26}Mg/^{24}Mg ratio for a single measurement of one block of 40 ratios is less than ±0.02‰ (2SD). The internal precision on the measured ^{26}Mg/^{24}Mg ratio, based on ⩾4 repeat runs of the same sample solution

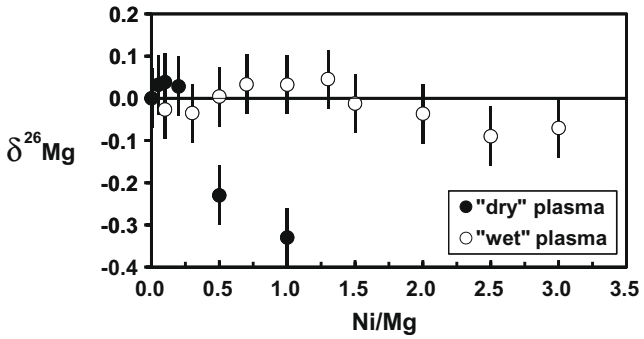

Fig. 2. Effect of Ni on Mg isotopic analysis. The instrumental mass bias for Mg isotopes is not affected by the presence of Ni with Ni/Mg concentration ratio up to 2 for "wet" plasma, under which data were acquired in this study, but is significant for "dry" plasma. The Ni/Mg ratios of all chondrites analyzed here are less than 0.3. Error bars in this and all later figures represent 2SD uncertainties.

during a single analytical session, was better than ±0.1‰ (2SD). The external precision, as shown by replicate analyses of synthetic solution, mineral and rock standards, was ~±0.06‰ for δ^{25}Mg and ~±0.07‰ for δ^{26}Mg (2SD). Given that analysis of ^{26}Mg/^{24}Mg ratios yields ‰/amu precision better than ^{25}Mg/^{24}Mg ratios, δ^{26}Mg values are used in the discussion. Some studies of high-precision Mg isotopic analyses have reported uncertainties by standard error (SE) of the mean ($2SE = 2SD/\sqrt{n}$, where n is the number of replicate analyses). The uncertainties reported here are the standard deviation (2SD) based on n replicate analyses. One should take uncertainties on averages of large sample populations as provisional, as accuracy was tested down to the level of the long-term external precision. When the uncertainties on averages of large sample populations are better than 0.07‰ for δ^{26}Mg, the long-term external precision of 0.07‰ is applied here.

Multiple analyses of IL-Mg-1, a synthetic multi-element standard solution with concentration ratios of Mg:Fe:Al:Ca:Na:K:Ti = 1:1:1:1:1:1:0.1, yielded δ^{25}Mg values of −0.05 to +0.05, with an average value of −0.01 ± 0.06 and δ^{26}Mg values of −0.07 to +0.05, with an average value of −0.01 ± 0.07 (2SD, $n = 13$) (Fig. 3). This is in agreement with the expected value of 0 and shows that our data are accurate within a precision of ±0.06‰ for δ^{25}Mg and ±0.07‰ for δ^{26}Mg. An olivine sample from Kilbourne Hole was also analyzed multiple times. The δ^{26}Mg values range from −0.36 to −0.23, with an average value of −0.27 ± 0.07 (2SD, $n = 16$) (Fig. 3). This agrees with published data of −0.31 ± 0.09 (2SD) (Teng et al., 2007). Furthermore, SUNY MORB, an in-house basalt standard used in previous studies (Teng et al., 2007; Richter et al., 2008), was analyzed here and yielded similar Mg isotopic composition to published data (−0.23 ± 0.06 vs. −0.28 ± 0.06, 2SD). Finally, data measured in this study are consistent with published data for Cambridge-1 (Galy et al., 2003), seawater (Young and Galy, 2004), Allende carbonaceous chondrite (see Teng et al., 2007 for compilation of published data of Allende) and dunite DTS-2 (Huang et al., 2009).

When compared to previous studies of Allende, Murchison, SUNY MORB and Kilauea Iki lavas (Teng et al., 2007), the data reported in this paper agree within external uncertainty, but are systematically heavier by up to 0.1‰. For example, the δ^{26}Mg values of samples from Kilauea Iki lava lake vary from −0.30 to −0.18 with an average value of −0.26 ± 0.06 (2SD) in this study, whereas Teng et al. (2007) reported variations from −0.42 to −0.26 with an average value of −0.36 ± 0.06 (2SD) (Fig. 4). The ⩽0.1‰ difference reflects a systematic inter-laboratory bias. Tests of accuracy suggest that the data presented here are more accurate than those reported by Teng et al. (2007). For example, δ^{26}Mg values of synthetic solutions that were made by mixing DSM3 with San Carlos olivine matrix and Allende matrix in Teng et al. (2007) were −0.10 ± 0.10 (2SD, expected value = 0), whereas those of IL-Mg-1 analyzed here are −0.01 ± 0.07 (2SD). Therefore, the data collected here supersede previously published values and will be used in the discussion.

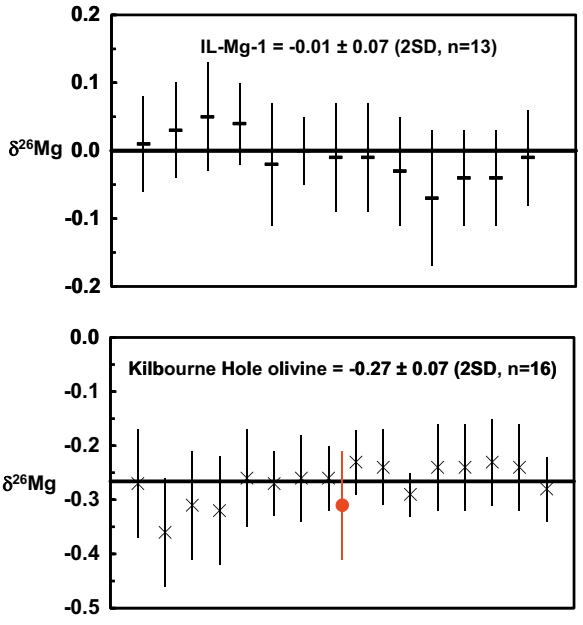

Fig. 3. Upper panel: Measured Mg isotopic compositions of a synthetic solution with concentration ratios of Mg:Fe:Al:Ca:Na:K:Ti = 1:1:1:1:1:1:0.1. Lower panel: Mg isotopic compositions of Kilbourne Hole olivine analyzed during the course of this study. Solid lines in both panels represent the average values and red circle in the lower panel represents published value for Kilbourne Hole olivine (Teng et al., 2007). Data are from Table 1. (For interpretation of the references to color in this figure legend, the reader is referred to the web version of this article.)

4. RESULTS

Magnesium isotopic compositions are reported in Table 1 for reference samples, Table 2 for MORBs, Table 3 for OIBs, Table 4 for peridotite xenoliths and Table 5 for chondrites. All natural samples including chondrites analyzed in this study fall on a single isotopic mass-dependent fractionation line with a slope of 0.515 (Fig. 5). This slope corresponds to the same value in a δ^{26}Mg′ and δ^{25}Mg′ plot. (See Young and Galy (2004) for definition of the δ^{26}Mg′ and δ^{26}Mg′ notations.)

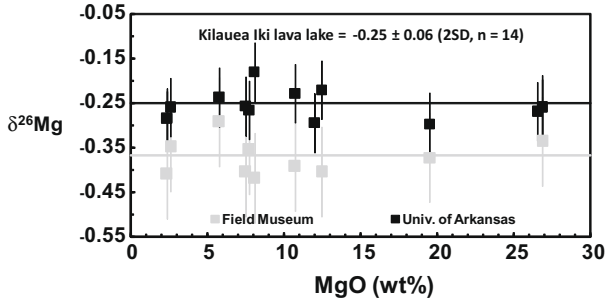

Fig. 4. Absence of Mg isotope fractionation during magmatic differentiation of Kilauea Iki lava lake. Dark (light) solid line represents the average δ^{26}Mg of all samples measured at the University of Arkansas (Field Museum). Data are from Table 3 and Teng et al. (2007). The new data are taken to be more accurate and supersede previous values.

Table 2
Magnesium isotopic compositions of MORBs ($n = 47$).

Sample	Type	MgO (wt%)	δ^{25}Mg	2SD	δ^{26}Mg	2SD
Mid-Atlantic Ridge						
CH31 DR01	E	8.97	−0.12	0.06	−0.23	0.07
CH31 DR02	E	7.93	−0.15	0.05	−0.29	0.07
CH31 DR11	E	8.36	−0.13	0.05	−0.27	0.07
CH31 DR12	E	7.7	−0.12	0.05	−0.24	0.07
CH98 DR08	N		−0.12	0.05	−0.23	0.07
CH98 DR12	N	7.69	−0.11	0.06	−0.25	0.07
CH98 DR15	N	8.43	−0.14	0.05	−0.29	0.07
CH98 DR17	N	7.77	−0.16	0.06	−0.31	0.07
East Pacific Rise						
CL DR01	N	8.15	−0.11	0.06	−0.25	0.07
CY82-21-06	T	8.04	−0.14	0.05	−0.25	0.07
CY82-31-02V	N	8.52	−0.12	0.05	−0.26	0.07
CY82-31-01	N	8.97	−0.18	0.05	−0.31	0.07
CY84-05-08	N	7.21	−0.11	0.05	−0.23	0.07
SO40 G136D	N	7.64	−0.17	0.08	−0.26	0.09
SO40 G178D	N	7.92	−0.12	0.06	−0.24	0.08
SO40 G154D	N	7.89	−0.08	0.06	−0.20	0.08
SO40 G193h	N	7.3	−0.10	0.05	−0.20	0.08
SO26 G184D	N	7.03	−0.15	0.08	−0.28	0.09
SO62 G324G	N	6.41	−0.19	0.06	−0.30	0.08
SO62 G296G	N	7.88	−0.14	0.04	−0.25	0.05
SO62 G287G	N	7.92	−0.10	0.06	−0.22	0.08
SR1 DR04	N	6.99	−0.13	0.05	−0.25	0.08
SR2 DR02	N	7.33	−0.14	0.04	−0.26	0.06
SR2 DR03	N	7.3	−0.15	0.05	−0.29	0.08
SR2 DR-7			−0.14	0.06	−0.30	0.08
ND12-2	N	7.51	−0.14	0.06	−0.29	0.08
ND15-4	N	7.31	−0.11	0.06	−0.21	0.08
ND18-1	T	6.9	−0.11	0.06	−0.23	0.08
ND21-3	N	7.36	−0.14	0.04	−0.24	0.06
ND21-4	N	8.04	−0.13	0.05	−0.23	0.08
Indian Ocean Ridge						
HY09-07	N	8.09	−0.17	0.06	−0.28	0.07
JC 030703 D1	N	7.86	−0.17	0.05	−0.28	0.07
JC 217 D1	N	7.53	−0.13	0.06	−0.25	0.08
MD57 D4-4	N	8.53	−0.12	0.04	−0.23	0.06
MD57 D9-9	N	9.73	−0.13	0.04	−0.24	0.05
MD22-3	N		−0.15	0.05	−0.31	0.07
MD23-1	N	7.38	−0.10	0.04	−0.22	0.05
MD23-2	T		−0.17	0.05	−0.31	0.07
MD23 site-2	T	8.53	−0.11	0.04	−0.23	0.05
MD23 site-4	T	8.63	−0.12	0.05	−0.24	0.07
Red Sea						
KS11A	E	6.9	−0.12	0.05	−0.22	0.08
MR80 57-1	T	7.9	−0.16	0.06	−0.26	0.08
MR80 59-2	T	8.4	−0.09	0.06	−0.19	0.08
MR80 59-4			−0.15	0.06	−0.25	0.08
North Fiji Basin						
ST2-17-6	T	7.46	−0.10	0.04	−0.23	0.06
ST2-17-7	N	7.31	−0.11	0.04	−0.21	0.06
ST2-17-10	T	7.4	−0.10	0.04	−0.22	0.06

See Table 1 caption for notations and error bar calculations. E, enriched MORB; N, normal MORB; and T, transitional MORB. MgO data are from Marty and Zimmermann (1999).

The Mg isotopic compositions of global oceanic basalts display limited variations. δ^{26}Mg range from −0.31 to −0.19 (average = −0.25 ± 0.06, 2SD, $n = 47$) in global MORBs (Fig. 6) and −0.35 to −0.18 (average = −0.26 ± 0.08, 2SD, $n = 63$) in OIBs including Kilauea Iki lavas (Fig. 7). Correspondingly, δ^{25}Mg range from −0.19 to −0.08 (average = −0.13 ± 0.05) in global MORBs and −0.19 to −0.09 (average −0.13 ± 0.04) in OIBs. These

Table 3
Magnesium isotopic compositions of OIBs ($n = 63$).

Sample	MgO (wt%)	δ^{25}Mg	2SD	δ^{26}Mg	2SD
Society Island and Cook-Austral chain, French Polynesian					
DTH 02-01	0.86	−0.15	0.05	−0.29	0.09
DTH 02-02	0.86	−0.15	0.05	−0.31	0.10
DTH 03-03	9.16	−0.12	0.06	−0.26	0.08
DTH 04-01	0.91	−0.15	0.05	−0.28	0.09
DTH 04-04		−0.18	0.06	−0.34	0.08
Replicate		−0.20	0.06	−0.32	0.08
DTH 05-02	0.68	−0.15	0.08	−0.26	0.09
SO47 34DS-1	8.06	−0.16	0.06	−0.33	0.08
SO47 37GC		−0.18	0.06	−0.31	0.08
SO47 9DS	9.91	−0.14	0.04	−0.31	0.05
SO47 5DS-1	8.28	−0.12	0.06	−0.26	0.08
SO47 81DS3		−0.10	0.06	−0.22	0.08
Replicate		−0.13	0.05	−0.25	0.10
TH09-02	10.11	−0.15	0.04	−0.25	0.06
TH09-05	8.78	−0.13	0.08	−0.26	0.09
TH07-02		−0.13	0.06	−0.27	0.09
TH11-01	7.54	−0.13	0.05	−0.26	0.08
TH12-01	9.74	−0.16	0.04	−0.30	0.07
Replicate		−0.10	0.06	−0.24	0.09
TH12-06	4.67	−0.18	0.06	−0.35	0.09
Replicate		−0.15	0.08	−0.27	0.09
TH14-02	4.53	−0.14	0.08	−0.32	0.09
TH14-03	4.8	−0.12	0.06	−0.24	0.09
TH14-05	4.91	−0.15	0.04	−0.30	0.06
TH10-04	9.26	−0.13	0.08	−0.26	0.09
TH21	6.31	−0.16	0.06	−0.30	0.09
TH25-03	1.19	−0.19	0.06	−0.34	0.08
Replicate		−0.17	0.06	−0.31	0.10
TH28-07	7.23	−0.13	0.06	−0.30	0.08
TH30-03	5.53	−0.12	0.05	−0.26	0.07
Koolau, Hawaii					
KOO-7	6.99	−0.12	0.06	−0.20	0.07
Replicate		−0.11	0.05	−0.22	0.07
KOO-8	7.25	−0.17	0.05	−0.29	0.07
KOO-10	10.71	−0.11	0.08	−0.24	0.09
Replicate		−0.07	0.05	−0.23	0.07
KOO-15	7.08	−0.13	0.05	−0.22	0.07
Replicate		−0.10	0.06	−0.19	0.07
KOO-17	8.86	−0.12	0.05	−0.22	0.07
KOO-17A	19.0	−0.10	0.05	−0.21	0.07
KOO-19	6.58	−0.09	0.05	−0.18	0.07
KOO-21	9.26	−0.14	0.05	−0.26	0.07
KOO-24	8.81	−0.14	0.05	−0.24	0.07
KOO-32	9.21	−0.12	0.05	−0.26	0.07
KOO-48	6.84	−0.09	0.05	−0.19	0.07
KOO-49	10.15	−0.10	0.05	−0.19	0.07
KOO-55	8.35	−0.10	0.05	−0.18	0.07
KOO-55D	10.44	−0.12	0.05	−0.24	0.07
Replicate		−0.13	0.05	−0.25	0.07
Replicate		−0.13	0.04	−0.26	0.07
OH-21	6.83	−0.12	0.05	−0.22	0.07
OH-22	6.76	−0.12	0.05	−0.22	0.07
OH-24	6.79	−0.12	0.05	−0.26	0.07
OH-25	7.04	−0.10	0.08	−0.23	0.09
Replicate		−0.12	0.05	−0.24	0.07
OH-26	6.72	−0.10	0.05	−0.23	0.07
OH-27	6.28	−0.13	0.05	−0.21	0.07
KM-1	13.57	−0.13	0.06	−0.27	0.08
KM-3	12.64	−0.13	0.06	−0.28	0.08

(*continued on next page*)

Table 3 (*continued*)

Sample	MgO (wt%)	δ^{25}Mg	2SD	δ^{26}Mg	2SD
Kilauea Iki lava lake, Hawaii					
KI81-1-169.9	26.87	−0.12	0.05	−0.26	0.06
Replicate		−0.13	0.05	−0.26	0.07
KI81-1-239.9	26.55	−0.13	0.04	−0.27	0.07
IKI-22	19.52	−0.12	0.05	−0.30	0.07
KI75-1-38.9	12.46	−0.13	0.04	−0.22	0.07
KI67-3-27.5	12.01	−0.14	0.04	−0.29	0.07
KI75-1-139.3	11.70	−0.11	0.03	−0.24	0.04
KI67-3-39	10.73	−0.11	0.04	−0.23	0.07
IKI-58	8.08	−0.11	0.04	−0.18	0.07
KI67-3-81	7.73	−0.13	0.04	−0.27	0.07
KI75-1-121.5	7.5	−0.11	0.04	−0.26	0.07
KI75-1-75.2	5.77	−0.12	0.04	−0.24	0.07
KI67-2-85.7	2.60	−0.12	0.04	−0.26	0.07
KI81-2-88.6	2.37	−0.20	0.05	−0.29	0.06
Replicate		−0.15	0.04	−0.28	0.07
KI81-5-254.5		−0.12	0.03	−0.26	0.04
Loihi, Hawaii					
T4D4-01		−0.12	0.03	−0.24	0.04
T4D2#1		−0.12	0.03	−0.29	0.04
Replicate		−0.14	0.03	−0.26	0.04

See Table 1 caption for notations and error bar calculations. MgO data are from Helz et al. (1994), Frey et al. (1994), Norman and Garcia (1999) and measured for this study.

values fall within the range of the few previously reported values for oceanic basalts (Wiechert and Halliday, 2007).

Global peridotites with different mineralogy and chemical composition have homogenous Mg isotopic compositions. The δ^{26}Mg values vary from −0.28 to −0.21 with an average value of -0.25 ± 0.04 (2SD, $n = 29$) (Fig. 8) and δ^{25}Mg values vary from −0.16 to −0.09 with an average value of -0.13 ± 0.03. These values fall within the range of peridotite minerals (pyroxene and olivine) reported in previous studies (Handler et al., 2009; Yang et al., 2009; Young et al., 2009), but are lighter (by 0.2‰ in δ^{26}Mg) than those reported in Wiechert and Halliday (2007).

Magnesium isotopic compositions of 38 chondrites that cover 9 chondrite groups and 7 petrologic grades are indistinguishable within uncertainties, with δ^{26}Mg values between −0.35 and −0.23 and an average value of -0.28 ± 0.06 (2SD) (Fig. 9) and δ^{25}Mg values between −0.19 and −0.11 and an average value of -0.15 ± 0.04. Different types of sample dissolution methods applied to Allende and Murchison yield consistent Mg isotopic compositions, suggesting that no bias was introduced by using different types of dissolution or by processing the samples on TODGA resin to remove Ca and REEs (Pourmand and Dauphas, 2010). Samples processed through both Ti column chemistry and Mg column chemistry have similar Mg isotopic compositions to those that were only processed through the Mg column chemistry, suggesting our main-Mg column chemistry can quantitatively remove Ti from Mg. Our values, however, are in sharp contrast to published δ^{26}Mg data for 11 chondrites, which vary substantially from −0.49 to +0.06 (Table 5).

5. DISCUSSION

The similar δ^{26}Mg value for each group of mantle rocks and all types of chondrites is surprising, considering the diversity of the analyzed samples. In this section, we first discuss the behavior of Mg isotopes during partial melting and basaltic differentiation, then use the data collected here to calculate the average Mg isotopic composition of the Earth and chondrites, and finally evaluate the potential implications of the chondritic Mg isotopic composition of the Earth on the early history of the solar system.

5.1. Magnesium isotopic composition of the mantle

The globally distributed and chemically diverse oceanic basalts have identical Mg isotopic composition within uncertainties, with an average $\delta^{25}\text{Mg} = -0.13 \pm 0.05$ and average $\delta^{26}\text{Mg} = -0.26 \pm 0.07$ (2SD, $n = 110$). Similarly, peridotite samples investigated here vary in terms of location, origin, degree of partial melting and metasomatism, petrology, mineralogy as well as chemical and radiogenic isotopic composition. Their Mg isotopic compositions, however, are uniform ($\delta^{25}\text{Mg} = -0.13 \pm 0.03$; $\delta^{26}\text{Mg} = -0.25 \pm 0.04$, 2SD, $n = 29$) (Fig. 8) and are similar to those of peridotite minerals investigated by Handler et al. (2009) and Yang et al. (2009), and those of komatiites from Alexo, Ontario, Canada, which were formed by 50% partial melting of the deep mantle in the Archean (Dauphas et al., 2010).

The similarity of Mg isotopic compositions between these peridotites and oceanic basalts suggests a lack of significant equilibrium Mg isotope fractionation during partial melting of mantle peridotites and basalt differentiation. This is consistent with studies of the Kilauea Iki lava lake that suggest basalt differentiation does not fractionate Mg isotopes (Teng et al., 2007). A similar conclusion is drawn when our findings are compared with studies of coexisting olivines and pyroxenes in peridotite xenoliths from global locations, which suggest that no measurable Mg isotope

Table 4
Magnesium isotopic compositions of peridotite xenoliths ($n = 29$).

Sample	Location	Rock type	MgO (wt%)	Mg#	δ^{25}Mg	2SD	δ^{26}Mg	2SD
New Mexico, USA								
KH-1	Kilbourne Hole	Lherzolite	39.1	90.1	−0.15	0.06	−0.26	0.08
Po-1	Potrillo	Lherzolite	38.3	89.5	−0.15	0.06	−0.28	0.08
France								
Fr-1	Massif Central	Lherzolite	38.0	90.1	−0.15	0.06	−0.25	0.08
Australia								
2728	Gambier	Lherzolite	43.43	91.7	−0.14	0.05	−0.23	0.09
84438	Shadwell	Lherzolite			−0.16	0.05	−0.27	0.09
Northern Tanzania								
89-675	Lashaine	Harzburgite	45.3	92.6	−0.11	0.05	−0.26	0.05
89-661	Lashaine	Lherzolite	47.7	93.3	−0.13	0.05	−0.25	0.05
89-662	Lashaine	Dunite	48.8	91.8	−0.12	0.05	−0.25	0.05
89-664	Lashaine	Harzburgite	46.9	89.9	−0.14	0.05	−0.26	0.05
89-672	Lashaine	Dunite	49.6	92.6	−0.11	0.05	−0.23	0.05
89-674	Lashaine	Lherzolite	44.9	91.4	−0.13	0.05	−0.26	0.05
89-719	Lashaine	Harzburgite	46.6	92.9	−0.12	0.05	−0.22	0.05
89-772	Olmani	Dunite	46.1	86.8	−0.14	0.05	−0.23	0.08
Replicate					−0.14	0.05	−0.26	0.09
89-773	Olmani	Harzburgite	49.1	93.6	−0.13	0.05	−0.26	0.06
89-774	Olmani	Dunite	51.9	93.7	−0.11	0.05	−0.22	0.06
89-777	Olmani	Wehrlite	48.2	91.0	−0.11	0.05	−0.23	0.06
89-780	Olmani	Dunite	51.0	93.1	−0.12	0.05	−0.26	0.06
LB-45	Labait	Lherzolite	38.7	89.2	−0.10	0.04	−0.21	0.09
Replicate					−0.13	0.04	−0.21	0.09
LB-49	Labait	Glimmerite			−0.13	0.05	−0.26	0.06
North China craton								
HY1-01	Kuandian	Harzburgite	44.5	90.5	−0.11	0.05	−0.24	0.06
HY2-01	Kuandian	Lherzolite	41.7	89.7	−0.14	0.05	−0.23	0.06
HY2-02	Kuandian	Lherzolite	40.2	88.7	−0.14	0.05	−0.26	0.06
HY2-03	Kuandian	Lherzolite	41.2	89.2	−0.12	0.05	−0.23	0.09
Replicate					−0.12	0.05	−0.23	0.08
Replicate					−0.14	0.06	−0.27	0.08
HY2-04	Kuandian	Lherzolite	40.7	88.5	−0.15	0.05	−0.27	0.08
HY2-05	Kuandian	Harzburgite	45.8	90.5	−0.12	0.05	−0.23	0.08
HY2-06	Kuandian	Lherzolite	38.4	88.4	−0.15	0.05	−0.27	0.08
HY2-07	Kuandian	Lherzolite	38.4	88.5	−0.10	0.05	−0.21	0.08
HY2-14	Kuandian	Lherzolite	42.4	89.8	−0.12	0.05	−0.25	0.08
HY2-29	Kuandian	Lherzolite	38.6	88.4	−0.09	0.05	−0.22	0.08

See Table 1 caption for notations and error bar calculations. Mg# = 100 × atomic ratio Mg/(Mg + Fe). MgO contents are from Frey and Green (1974), Jagoutz et al. (1979), Rudnick et al. (1993, 1994) and Wu et al. (2006). Whole-rock Mg# of Lashaine samples is calculated from Mg# of minerals and modal mineralogy of whole rocks (Rudnick et al., 1994). Mg# for other samples is directly calculated from the chemical compositions of the whole rocks.

fractionation occurred at mantle temperatures within ~±0.1‰ (Handler et al., 2009; Yang et al., 2009).

Given that MORBs sample the asthenosphere, OIBs sample greater depths of the mantle, and the peridotites sample the continental lithosphere, the indistinguishable Mg isotopic compositions of global MORBs, OIBs and peridotites suggest a homogenous Mg isotopic composition of the mantle, at least at the whole-rock scale, with $\delta^{25}Mg = -0.13 \pm 0.04$ and $\delta^{26}Mg = -0.25 \pm 0.07$ (2SD, $n = 139$) (Fig. 10).

5.2. Magnesium isotopic composition of chondrites

Chondrites have variable petrological, mineralogical, chemical and isotopic compositions that reflect inheritance from the solar system parent molecular cloud, conditions in the protosolar nebula, and parent body processes (e.g., Scott and Krot, 2003). Whether these processes affected the abundances of non-traditional stable isotopes (e.g., Li, Mg, Si, Fe, etc.) in meteorites is the subject of considerable attention. For example, Li isotopes vary significantly among different types of chondrites, reflecting either isotope fractionation during aqueous alteration and thermal metamorphism of parent bodies of chondrites (McDonough et al., 2003), or irradiation processes in the protosolar nebula (Seitz et al., 2007). Similarly, recent study of Si isotopes (Fitoussi et al., 2009) has also found that chondrites have variable Si isotopic compositions, with a systematic increase towards heavier isotopic composition with increasing Mg/Si ratio (Fitoussi et al., 2009). This has been interpreted

Table 5
Magnesium isotopic compositions of chondrites ($n = 38$).

Meteorite	Classification		$\delta^{25}Mg$	2SD	$\delta^{26}Mg$	2SD	$\delta^{26}Mg^*$	2SD
Carbonaceous								
Ivuna	CI1	Fall	−0.14	0.06	−0.24	0.07	0.03	0.14
Replicate			−0.18	0.06	−0.31	0.10	0.04	0.05
Replicate-Ti			−0.12	0.04	−0.26	0.07	−0.03	0.05
Mighei	CM2	Fall	−0.17	0.07	−0.25	0.09	0.08	0.09
Replicate			−0.16	0.06	−0.25	0.10	0.06	0.06
Murchison[a]	CM2	Fall	−0.17	0.03	−0.31	0.07	0.01	0.02
Kainsaz	CO3	Fall	−0.16	0.05	−0.28	0.09	0.03	0.05
Lancé	CO3	Fall	−0.19	0.06	−0.33	0.07	0.04	0.07
Replicate-Ti			−0.13	0.04	−0.24	0.07	0.01	0.09
Allende[a]	CV3	Fall	−0.15	0.04	−0.30	0.05	0.01	0.04
Grosnaja	CV3	Fall	−0.15	0.05	−0.27	0.09	0.02	0.07
Vigarano	CV3	Fall	−0.16	0.04	−0.32	0.07	−0.01	0.06
Replicate-Ti			−0.16	0.04	−0.28	0.07	0.03	0.05
Ordinary								
Bielokrynitschie	H4	Fall	−0.16	0.05	−0.30	0.09	0.01	0.04
Kesen	H4	Fall	−0.15	0.04	−0.25	0.07	0.04	0.05
Replicate[b]			−0.15	0.04	−0.30	0.07	−0.01	0.06
Ochansk	H4	Fall	−0.15	0.06	−0.29	0.07	0.00	0.07
Kernouve	H6	Fall	−0.13	0.06	−0.29	0.07	−0.04	0.05
Replicate-Ti			−0.15	0.04	−0.32	0.07	−0.03	0.06
Baratta	L4	Find	−0.15	0.04	−0.30	0.07	−0.01	0.08
Dalgety Downs	L4	Find	−0.18	0.06	−0.29	0.10	0.06	0.14
Replicate-Ti			−0.16	0.05	−0.26	0.05	0.05	0.03
Farmington	L5	Fall	−0.19	0.07	−0.35	0.09	0.02	0.13
Replicate			−0.18	0.06	−0.33	0.10	0.02	0.07
Replicate-Ti			−0.11	0.04	−0.26	0.07	−0.05	0.06
Harleton	L6	Fall	−0.16	0.07	−0.29	0.09	0.02	0.04
Hamlet	LL4	Fall	−0.09	0.07	−0.22	0.09	−0.04	0.14
Replicate			−0.13	0.06	−0.28	0.10	−0.03	0.07
Replicate-Ti			−0.10	0.04	−0.20	0.07	−0.01	0.04
Kelly	LL4	Find	−0.16	0.04	−0.30	0.07	0.01	0.07
Replicate-Ti			−0.16	0.05	−0.31	0.07	0.00	0.07
Soko-Banja	LL4	Fall	−0.17	0.05	−0.29	0.09	0.04	0.06
Paragould	LL5	Fall	−0.14	0.07	−0.27	0.09	0.00	0.07
Replicate-Ti			−0.14	0.05	−0.31	0.07	−0.04	0.05
Tuxtuac	LL5	Fall	−0.16	0.04	−0.28	0.07	0.03	0.11
Saint-Séverin	LL6	Fall	−0.13	0.07	−0.27	0.09	−0.02	0.05
Replicate-Ti			−0.13	0.05	−0.28	0.07	−0.03	0.03
Enstatite								
Qingzhen	EH3	Fall	−0.15	0.06	−0.28	0.07	0.01	0.06
Sahara 97072	EH3	Find	−0.15	0.06	−0.30	0.10	−0.01	0.09
Adhi Kot	EH4	Fall	−0.15	0.05	−0.26	0.09	0.03	0.06
Indarch	EH4	Fall	−0.15	0.07	−0.25	0.09	0.04	0.02
Replicate-Ti			−0.14	0.05	−0.30	0.07	−0.03	0.09
Saint-Sauveur	EH5	Fall	−0.14	0.05	−0.27	0.09	0.00	0.05
St. Mark's	EH5	Fall	−0.15	0.06	−0.30	0.07	−0.01	0.07
Replicate-Ti			−0.15	0.05	−0.29	0.07	0.00	0.08
Blithfield	EL6	Find	−0.16	0.04	−0.25	0.07	0.06	0.07
Daniel's Kuil	EL6	Fall	−0.15	0.06	−0.27	0.07	0.02	0.01
Eagle	EL6	Fall	−0.14	0.07	−0.27	0.09	0.00	0.14
Hvittis	EL6	Fall	−0.17	0.04	−0.29	0.07	0.04	0.13
Jajh deh Kot Lalu	EL6	Fall	−0.18	0.04	−0.34	0.07	0.01	0.17
Replicate-Ti			−0.16	0.05	−0.27	0.07	0.04	0.08
Khairpur	EL6	Fall	−0.14	0.06	−0.26	0.07	0.01	0.06
Pillistfer	EL6	Fall	−0.14	0.06	−0.31	0.07	−0.04	0.05
Replicate-Ti			−0.13	0.05	−0.27	0.07	−0.02	0.02
Yilmia	EL6	Find	−0.14	0.06	−0.28	0.10	−0.01	0.07
Happy Canyon	EL6/7	Find	−0.19	0.07	−0.33	0.09	0.04	0.04
Replicate			−0.18	0.06	−0.26	0.10	0.03	0.05
Replicate-Ti			−0.13	0.05	−0.28	0.07	−0.03	0.05

Table 5 (*continued*)

Meteorite	Classification		δ^{25}Mg	2SD	δ^{26}Mg	2SD	δ^{26}Mg*	2SD
Ilafegh 009	EL7	Find	−0.16	0.06	−0.33	0.10	−0.02	0.03
Replicate-Ti			−0.17	0.05	−0.32	0.07	0.01	0.09
Literature data								
Orgueil (WH)[b]	CI		−0.14	0.02	−0.32	0.06		
Orgueil (Y)	CI		−0.19		−0.37			
Orgueil (YG)	CI		−0.01	0.04	−0.03	0.06		
Murchison (B)	CM2		−0.14		−0.28			
Murchison (TWH)	CM2		−0.21	0.05	−0.41	0.05		
Murchison (WH)	CM2		−0.14	0.04	−0.26	0.07		
Murchison (YTZ)	CM2		−0.17	0.06	−0.31	0.06		
Allende (B)	CV3		−0.18		−0.36			
Allende (TWH)	CV3		−0.19	0.07	−0.37	0.06		
Allende (WH)	CV3		−0.13	0.04	−0.25	0.07		
Allende (Y)	CV3		−0.21		−0.39			
Allende (YG)	CV3		−0.16	0.03	−0.30	0.07		
Allende (YTZ)	CV3		−0.17	0.07	−0.28	0.10		
Bath (WH)	H4		−0.15	0.02	−0.34	0.06		
Allegan (WH)	H5		−0.11	0.04	−0.27	0.08		
Cangas de Onis (WH)	H5		−0.13	0.02	−0.24	0.07		
Cereseto (WH)	H5		−0.20	0.03	−0.49	0.04		
Épinal (WH)	H5		−0.14	0.03	−0.34	0.08		
Julesburg (B)	L3		0.01		−0.01			
Alfianello (B)	L6		0.03		0.06			
Bruderheim (WH)	L6		−0.20	0.04	−0.41	0.06		

See Table 1 caption for notations and error bar calculations. δ^{26}Mg* represents non-mass-dependent anomaly in the ^{26}Mg/^{24}Mg ratio due to the decay of ^{26}Al and was calculated as in Davis et al. (2005) (i.e., using a slope of 0.514 on a plot of ϕ^{25}Mg vs. ϕ ^{26}Mg, see Davis et al. (2005) for definitions and details).

[a] Mg isotopic compositions of Allende and Murchison are the average values from Table 1. Replicate-Ti: samples were processed through Ti-removal column before through the main-Mg column.

[b] Uncertainties from WH represent two standard error. B, Baker et al. (2005); TWH, Teng et al. (2007); WH, Wiechert and Halliday (2007); Y, Young et al. (2009); YTZ, Yang et al. (2009); and YG, Young and Galy (2004).

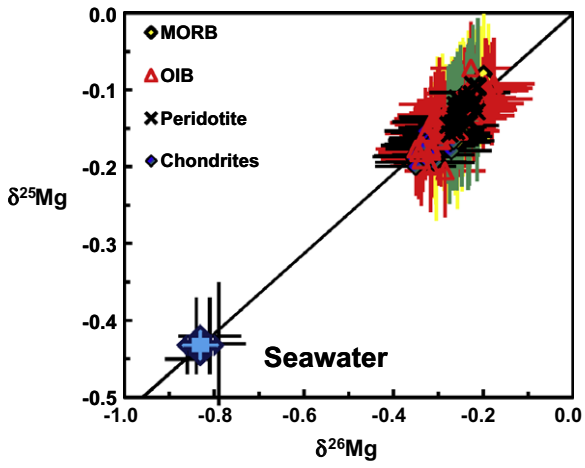

Fig. 5. Magnesium three-isotope plot of all natural samples analyzed in this study. The solid line represents the fractionation line with a slope of 0.515. Data are from Tables 1–5.

to result from reactions between olivine and a SiO-rich, isotopically light, vapor, producing enstatite in the solar nebula. In contrast to Li and Si isotopes, Fe isotopes are uniform in chondrites (e.g., Poitrasson et al., 2005; Schoenberg and von Blanckenburg, 2006; Dauphas et al., 2009a).

One of the three isotopes of Mg, ^{26}Mg, is also the decay product of a short-lived radioactive nuclide ^{26}Al ($t_{1/2} = 0.72$ Ma) (Lee et al., 1976, 1977). There is clear evidence of live ^{26}Al in the early solar system, as shown by the wide occurrence of radiogenic ^{26}Mg in CAIs and chondrules (Lee et al., 1976, 1977; Kita et al., 2005; Jacobsen et al., 2008). The meteorites analyzed here cover the whole spectrum of ^{27}Al/^{24}Mg ratios in chondrites, from ~0.08 to ~0.14 (Wasson and Kallemeyn, 1988; Hutchison, 2004). For an initial ^{26}Al/^{27}Al ratio of 5×10^{-5}, this would correspond to Δ^{26}Mg (see Table 5 for the definition of Δ^{26}Mg) of ~0.03 to ~0.05. As shown in Fig. 9c, such small variations cannot be resolved at our current analytical precision (~0.07 for Δ^{26}Mg, 2SD).

In addition to the production of ^{26}Mg from the decay of ^{26}Al, Mg isotopes also display large mass-dependent fractionations in chondrules and CAIs, mainly due to kinetic isotope fractionation associated with condensation and evaporation in the protosolar nebula (Clayton et al., 1988; Richter et al., 2002). In contrast to previous studies, based on a limited number of chondrite samples examined that show >0.5‰ variation in δ^{26}Mg (Young and Galy, 2004; Baker et al., 2005; Teng et al., 2007; Wiechert and

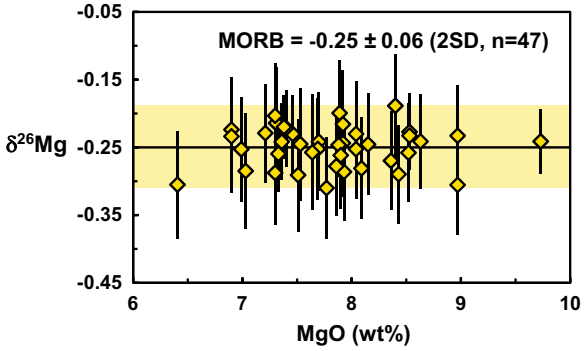

Fig. 6. δ^{26}Mg vs. MgO in global MORBs. Solid line and yellow bar represent the average δ^{26}Mg and two standard deviation of the average δ^{26}Mg of all MORBs, respectively. Data are from Table 2. (For interpretation of the references to color in this figure legend, the reader is referred to the web version of this article.)

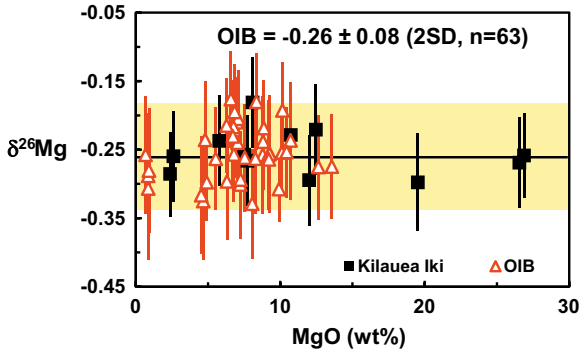

Fig. 7. δ^{26}Mg vs. MgO in OIBs. Solid line and yellow bar represent the average δ^{26}Mg and two standard deviation of the average δ^{26}Mg of all OIBs, respectively. Samples from Loihi are not plotted due to the lack of MgO contents. Data are from Table 3. (For interpretation of the references to color in this figure legend, the reader is referred to the web version of this article.)

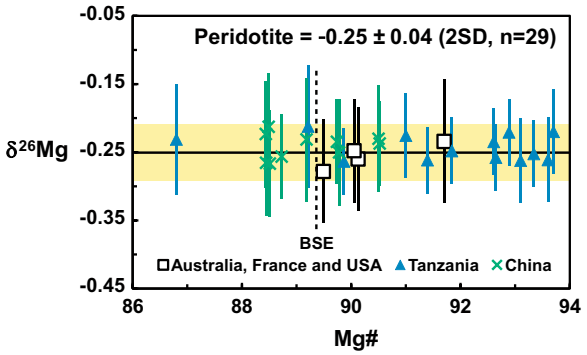

Fig. 8. δ^{26}Mg vs. Mg# in global peridotite xenoliths. Horizontal solid line and yellow bar represent the average δ^{26}Mg and two standard deviation of the average δ^{26}Mg of all peridotites, respectively. Vertical dashed line represents Mg# of the bulk silicate Earth (BSE) (Mg# = 89.3, McDonough and Sun, 1995). Data are from Table 4. (For interpretation of the references to color in this figure legend, the reader is referred to the web version of this article.)

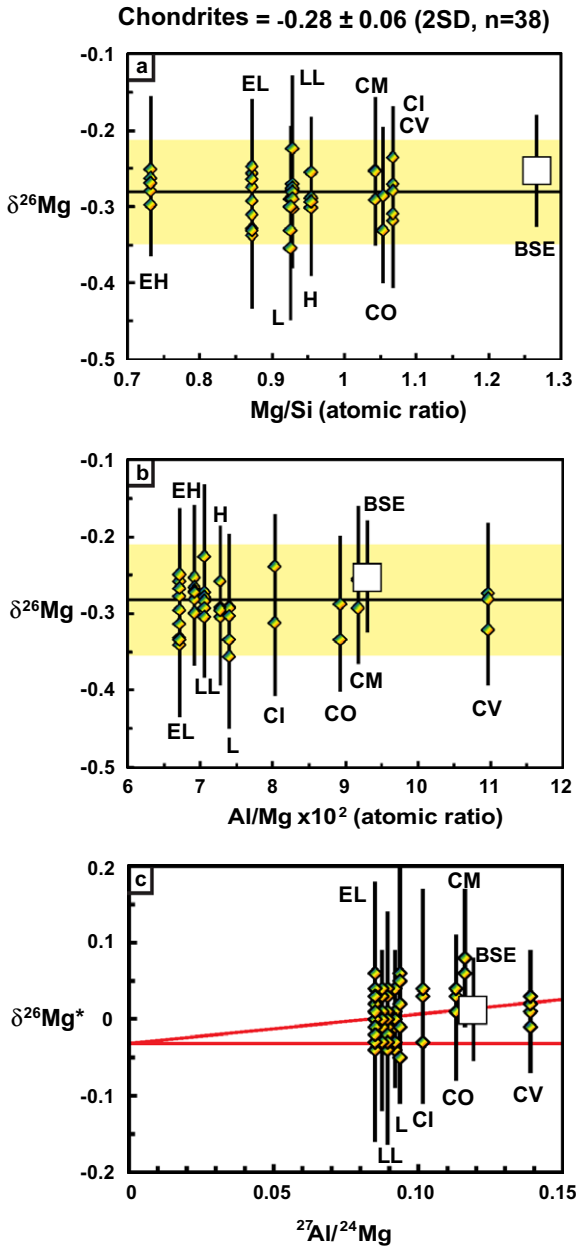

Fig. 9. δ^{26}Mg vs. average atomic Mg/Si ratio (a); δ^{26}Mg vs. average Al/Mg $\times$ 10^2 ratio (b) and δ^{26}Mg* vs. average ^{27}Al/^{24}Mg ratio (c) for all chondrites analyzed here. Horizontal lines and yellow bars in panels (a) and (b) represent the average δ^{26}Mg and two standard deviation of the average δ^{26}Mg of all chondrites. The two red lines in panel (c) correspond to initial ^{26}Al/^{27}Al ratios of 0 and 5 $\times$ 10^{-5}. Magnesium isotopic data are from Table 5 and average Mg/Si, Al/Mg and ^{27}Al/^{24}Mg ratios of chondrites are from Hutchison (2004). δ^{26}Mg of the bulk silicate Earth (BSE) is estimated to be -0.25 ± 0.07 (Fig. 10). The atomic Mg/Si, Al/Mg and ^{27}Al/^{24}Mg ratios of the BSE are from McDonough and Sun (1995). (For interpretation of the references to color in this figure legend, the reader is referred to the web version of this article.)

Halliday, 2007; Yang et al., 2009; Young et al., 2009), δ^{26}Mg and δ^{25}Mg values in all major types of chondrites analyzed here are constant and do not vary with chemical

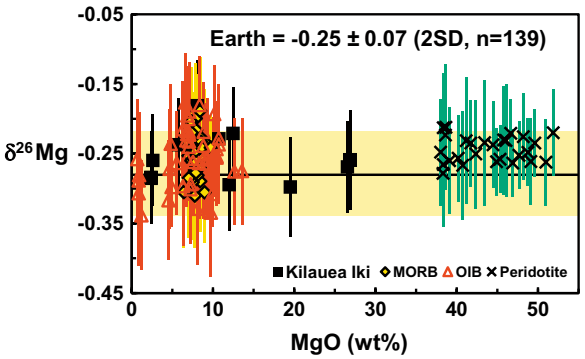

Fig. 10. Estimate of Mg isotopic composition of the Earth based on oceanic basalts and peridotites investigated here. The solid line and yellow bar represent the average δ^{26}Mg of −0.28 and two standard deviation of ±0.07 for all chondrites analyzed here. Data are from Tables 2–5. (For interpretation of the references to color in this figure legend, the reader is referred to the web version of this paper.)

compositions (e.g., Mg/Si and Al/Mg ratios) (Fig. 9). This difference may reflect Mg isotopic heterogeneity in chondrites, as CAIs and chondrules have different Mg isotopic compositions (Clayton et al., 1988; Richter et al., 2002). Alternatively, the observed discrepancies may be the result of analytical artifacts. The homogenous Mg isotopic composition of chondrites observed in this study suggests that Mg isotopes did not fractionate during processes in the solar system parent molecular cloud, in the protosolar nebula or on the parent bodies of chondrites, in a way that was similar to Fe isotopes but different from the isotopes of Li and Si.

5.3. Chondritic Mg isotopic composition of the Earth and implications

It is still highly debated whether the Earth has a chondritic Mg isotopic composition. Wiechert and Halliday (2007) concluded that the δ^{26}Mg of the Earth is on average ~0.3‰ higher than that of chondrites and, therefore, the Earth has a non-chondritic Mg isotopic composition. This conclusion was supported by a recent study based on two mantle peridotites and two chondrites (Young et al., 2009). By contrast, other recent high-precision Mg isotopic studies, which were based on oceanic basalts and peridotites, as well as komatiites, suggest that the Earth and chondrites have identical Mg isotopic composition at precision levels of ±0.1‰ for ^{26}Mg/^{24}Mg ratio (Teng et al., 2007; Chakrabarti and Jacobsen, 2009; Handler et al., 2009; Yang et al., 2009; Dauphas et al., 2010).

Magnesium isotopic compositions of the mantle (i.e., Earth) estimated from this study are slightly heavier than those of chondrites (e.g., δ^{26}Mg = −0.25 vs. −0.28). However, they are indistinguishable within current analytical uncertainties (e.g., ±0.07) (Fig. 10), which suggests the Earth has a chondritic Mg isotopic composition. Furthermore, samples in this study cover a wide range of ages, from Archean peridotites to young peridotites and oceanic basalts, and show constant Mg isotopic composition. This, together with previous studies of peridotites of different ages (Handler et al., 2009; Yang et al., 2009) and Archean komatiites (Dauphas et al., 2010), suggests lack of secular change in Mg isotopic composition of the Earth's mantle since the Archean. This agrees with the fact that the mantle dominates the Mg budget of the Earth (>99% of Mg is in the mantle) and that continental crust formation and crustal recycling cannot shift δ^{26}Mg of the mantle more than 0.01‰, even if all crustal materials had δ^{26}Mg value as light as seawater (−0.8‰).

The chondritic Mg isotopic composition of the Earth and homogeneous and mass-dependent fractionation of Mg isotopes in all types of chondrites reveal that Mg isotopes have been well-mixed and were not fractionated by early solar system processes. The Earth and chondrites appear to have formed from a nebular reservoir of homogenous Mg isotopic composition of a large scale. This obviates the need for models that involve physical separation of early condensates and chondrules from volatile-rich planetary dust (e.g., Wiechert and Halliday, 2007) in order to explain the Mg isotopic composition of the Earth.

The bulk silicate Earth and other planetary bodies in the inner solar system are depleted in Mg and Si and have a lower Mg/Al ratio and enhanced Mg/Si ratio relative to CI chondrites (Ringwood, 1989). This geochemical signature resulted from a volatility-controlled process prior to accretion of the Earth, which led to depletion of elements more volatile than Si in the inner planet region, and condensation in the lower-temperature environment in the outer asteroid belt (Ringwood, 1989). The constant Mg isotopic composition of all types of chondrites and the Earth, thus, indicates that the same processes that have led to depletions in the moderately-volatile to volatile elements in the solar nebula did not fractionate Mg isotopes. Furthermore, these processes are not expected to fractionate isotopes of lithophile elements with similar volatility to Mg either.

6. CONCLUSIONS

This study presents the largest dataset of high-precision Mg isotopic data for terrestrial basalts, peridotites and chondrites to date. The following conclusions can be drawn:

(1) Globally distributed, chemically diverse MORBs, OIBs and peridotite xenoliths have homogeneous Mg isotopic compositions with δ^{25}Mg varying from −0.19 to −0.08 and an average value of −0.13 ± 0.04, and δ^{26}Mg varying from −0.35 to −0.18 and an average value of −0.25 ± 0.07 (2SD, n = 139). These results are taken to represent the Mg isotopic composition of the mantle (i.e., Earth).
(2) The lack of Mg isotopic variation in global MORBs, OIBs and peridotites suggests insignificant equilibrium Mg isotope fractionation during partial melting of peridotite mantle and fractional crystallization of basaltic magma.
(3) Carbonaceous, ordinary and enstatite chondrites from nine groups (CI, CM, CO, CV, L, LL, H, EH and EL) have homogenous Mg isotopic composi-

tions, with δ^{25}Mg ranging from −0.19 and −0.11 and an average value of -0.15 ± 0.04, and δ^{26}Mg ranging from −0.35 to −0.23 and an average value of -0.28 ± 0.07 (2SD, $n = 38$). This suggests that Mg isotopes were well-mixed in the early solar system.

(4) The Earth, as represented by the mantle, has a chondritic Mg isotopic composition.

ACKNOWLEDGMENTS

We are grateful for Bill McDonough and Roberta Rudnick for peridotite samples from Kilbourne Hole (KH-1), Potrillo (Po-1), Massif Central (Fr-1), Australia and Northern Tanzania, Roz Helz for samples from Kilauea Iki lava lake, Wei Yang, Sheng-Ao Liu, Frank Richter and Mini Wadhwa for discussions. Very constructive and detailed comments from Monica Handler, Paul Tomascak, Rich Walker and an anonymous reviewer are greatly appreciated. This work was supported by the NSF EAR-0838227 and Arkansas Space Grant Consortium – SW19002 to F.Z.T., NSF EAR-0820807, NASA NNX09AG59G, and a Packard fellowship to N.D.

REFERENCES

Baker J. A., Bizzarro M., Wittig N., Connelly J. and Haack H. (2005) Early planetesimal melting from an age of 4.5662 Gyr for differentiated meteorites. *Nature* **436**, 1127–1131.

Chakrabarti R. and Jacobsen S. B. (2009) A combined silicon and magnesium isotopic study of bulk meteorites and the Earth. In *40th Lunar and Planetary Science Conference* 2089 (abstr.).

Chauvel C., Hofmann A. W. and Vidal P. (1992) HIMU-EM: The French Polynesian connection. *Earth Planet. Sci. Lett.* **110**, 99–119.

Chesley J. T., Rudnick R. L. and Lee C. T. (1999) Re–Os systematics of mantle xenoliths from the East African Rift: age, structure, and history of the Tanzanian craton. *Geochim. Cosmochim. Acta* **63**(7–8), 1203–1217.

Clayton R. N., Hinton R. W. and Davis A. M. (1988) Isotopic variations in the rock-forming elements in meteorites. *Philos. Trans. R. Soc. Lond. A.* **325**, 483–501.

Dauphas N. et al. (2009a) Iron isotopes may reveal the redox conditions of mantle melting from Archean to Present. *Earth Planet. Sci. Lett.* **288**(1–2), 255–267.

Dauphas N., Pourmand A. and Teng F.-Z. (2009b) Routine isotopic analysis of iron by HR-MC-ICPMS: how precise and how accurate? *Chem. Geol.* **267**, 175–184.

Dauphas N., Teng F.-Z. and Arndt N. T. (2010) Magnesium and iron isotopes in 2.7 Ga Alexo komatiites: mantle signatures, no evidence for Soret diffusion, and identification of diffusive transport in zoned olivine. *Geochim. Cosmochim. Acta* **74**, 3274–3291.

Davis A. M. et al. (2005) Isotopic mass fractionation laws and the initial Solar System ^{26}Al/^{27}Al ratio. *Lunar and Planetary Science XXXVI* #2334.

Dewey C. et al. (1990) Active submarine volcanism on the Society hot spot swell: a geochemical study. *J. Geophys. Res.* **95**, 5049–5070.

Fitoussi C., Bourdon B., Kleine T., Oberli F. and Reynolds B. C. (2009) Si isotope systematics of meteorites and terrestrial peridotites: implications for Mg/Si fractionation in the solar nebula and for Si in the Earth's core. *Earth Planet. Sci. Lett.* **287**, 77–85.

Frey F. A., Garcia M. O. and Roden M. F. (1994) Geochemical characteristics of Koolau Volcano: implications of intershield geochemical differences among Hawaiian volcanoes. *Geochim. Cosmochim. Acta* **58**, 1441–1462.

Frey F. A. and Green D. H. (1974) The mineralogy, geochemistry and origin of lherzolite inclusions in Victorian basanites. *Geochim. Cosmochim. Acta* **38**, 1023–1059.

Galy A. et al. (2003) Magnesium isotope heterogeneity of the isotopic standard SRM980 and new reference materials for magnesium-isotope-ratio measurements. *J. Anal. At. Spectrom.* **18**(11), 1352–1356.

Garcia M. O., Foss D. J. P., West H. B. and Mahoney J. J. (1995) Geochemical and isotopic evolution of Loihi Volcano, Hawaii. *J. Petrol.* **36**, 1647–1674.

Garcia M. O., Jorgenson B. A., Mahoney J. J., Ito E. and Irving A. J. (1993) An evaluation of temporal geochemical evolution of Loihi summit lavas: results from Alvin submersible dives. *J. Geophys. Res.* **98**, 535–550.

Handler M. R., Baker J. A., Schiller M., Bennett V. C. and Yaxley G. M. (2009) Magnesium stable isotope composition of Earth's upper mantle. *Earth Planet. Sci. Lett.* **282**, 306–313.

Handler M. R., Bennett V. C. and Esat T. M. (1997) The persistence of off-cratonic lithospheric mantle: Os isotopic systematics of variably metasomatised southeast Australian xenoliths. *Earth Planet. Sci. Lett.* **151**(1–2), 61–75.

Haskins E. R. and Garcia M. O. (2004) Scientific drilling reveals geochemical heterogeneity within the Kóolau shield, Hawaíi. *Contrib. Mineral. Petrol.* **147**, 162–188.

Helz R. T. (1987) Differentiation behavior of Kilauea Iki lava lake, Kilauea Volcano, Hawaii: an overview of past and current work. In *Magmatic Processes: Physiochemical Principles* (ed. B. O. Mysen). Geochem. Soc. Spec. Publ. 1, pp. 241–258.

Helz R. T., Kirschenbaum H., Marinenko J. W., and Qian R. (1994) Whole rock analyses of core samples from the 1967, 1975, 1979 and 1981 drillings of Kilauea Iki lava lake, Hawaii. U.S. Geol. Survey Open File Report: 94-684.

Hofmann A. W. (2003) Sampling mantle heterogeneity through oceanic basalts: isotopes and trace elements. In *The Mantle and Core. Treatise on Geochemistry* (ed. R. W. Carlson). Elsevier-Pergamon, Oxford, pp. 61–101.

Huang F., Glessner J. J., Ianno A., Lundstrom C. C. and Zhang Z. (2009) Magnesium isotopic composition of igneous rock standards measured by MC-ICP-MS. *Chem. Geol.* **268**(1–2), 15–23.

Huang S. C. and Frey F. A. (2005) Recycled oceanic crust in the Hawaiian Plume: evidence from temporal geochemical variations within the Koolau Shield. *Contrib. Mineral. Petrol.* **149**(5), 556–575. doi:10.1007/s00410-005-0664-9.

Hutchison R. (2004) *Meteorites: A Petrologic, Chemical and Isotopic Synthesis. Cambridge Planetary Science, 2*. Cambridge University Press, Cambridge, 506pp.

Jacobsen B. et al. (2008) ^{26}Al–^{26}Mg and ^{207}Pb–^{206}Pb systematics of Allende CAIs: canonical solar initial ^{26}Al/^{27}Al ratio reinstated. *Earth Planet. Sci. Lett.* **272**, 353–364.

Jagoutz E. et al. (1979) The abundances of major, minor and trace elements in the earth's mantle as derived from primitive ultramafic nodules. In *Proceedings of the 10th Lunar Planetary Science Conference*, pp. 2031–2050.

Jochum K. P., McDonough W. F., Palme H. and Spettel B. (1989) Compositional constraints on the continental lithospheric mantle from trace-elements in spinel peridotite xenoliths. *Nature* **340**(6234), 548–550.

Kita N. T. et al. (2005) Constraints on the origin of chondrules and CAIs from short-lived and long-lived radionuclides (eds. A. N. Krot, E. R. D. Scott and B. Reipurth). Astronomical Society of the Pacific, San Francisco, CA, pp. 558–587.

Lassiter J. C. and Hauri E. H. (1998) Osmium-isotope variations in Hawaiian lavas: evidence for recycled oceanic lithosphere in the Hawaiian plume. *Earth Planet. Sci. Lett.* **164**(3–4), 483–496.

Lee C.-T. A. and Rudnick R. L. (1999). Compositionally stratified cratonic lithosphere: petrology and geochemistry of peridotite xenoliths from the Labait tuff cone, Tanzania. In *Proceedings of the 7th International Kimberlite Conference* (eds. J. J. Gurney and S. R. Richardson), pp. 503–521.

Lee T., Papanastassiou D. A. and Wasserburg G. J. (1976) Demonstration of Mg-26 excess in Allende and evidence for Al-26. *Geophys. Res. Lett.* **3**, 109–112.

Lee T., Papanastassiou D. A. and Wasserburg G. J. (1977) Aluminum-26 in early Solar System – fossil or fuel. *Astrophys. J.* **211**, L107–L110.

Marty B. and Dauphas N. (2003) The nitrogen record of crust–mantle interaction and mantle convection from Archean to present. *Earth Planet. Sci. Lett.* **206**(3–4), 397–410.

Marty B. and Humbert F. (1997) Nitrogen and argon isotopes in oceanic basalts. *Earth Planet. Sci. Lett.* **152**(1–4), 101–112.

Marty B. and Tolstikhin I. N. (1998) CO_2 fluxes from mid-ocean ridges, arcs and plumes. *Chem. Geol.* **145**(3–4), 233–248.

Marty B. and Zimmermann L. (1999) Volatiles (He, C, N, Ar) in mid-ocean ridge basalts: assessment of shallow-level fractionation and characterization of source composition. *Geochim. Cosmochim. Acta* **63**(21), 3619–3633.

McDonough W. F. and McCulloch M. T. (1987) The southeast Australian lithospheric mantle – isotopic and geochemical constraints on its growth and evolution. *Earth Planet. Sci. Lett.* **86**(2–4), 327–340.

McDonough W. F. and Sun S. S. (1995) The composition of the Earth. *Chem. Geol.* **120**(3–4), 223–253.

McDonough W. F. et al. (2003) Lithium isotopic composition of chondritic meteorites. *Lunar and Planetary Science XXXIV* #1931.

Moore J. G., Clague D. A. and Normark W. R. (1982) Diverse basalt types from Loihi seamount, Hawaii. *Geology* **10**, 88–92.

Norman M. D. and Garcia M. O. (1999) Primitive magmas and source characteristics of the Hawaiian plume: petrology and geochemistry of shield picrites. *Earth Planet. Sci. Lett.* **168**, 27–44.

Norman M. D., Yaxley G. M., Bennett V. C. and Brandon A. D. (2006) Magnesium isotopic composition of olivine from the Earth, Mars, Moon, and pallasite parent body. *Geophys. Res. Lett.* **33**(15), L15202. doi:10.1029/2006GL026446.

Pearson N. J., Griffin W. L., Alard O. and O'Reilly S. Y. (2006) The isotopic composition of magnesium in mantle olivine: records of depletion and metasomatism. *Chem. Geol.* **226**(3–4), 115–133.

Poitrasson F., Levasseur S. and Teutsch N. (2005) Significance of iron isotope mineral fractionation in pallasites and iron meteorites for the core–mantle differentiation of terrestrial planets. *Earth Planet. Sci. Lett.* **234**(1–2), 151–164.

Pourmand A. and Dauphas N. (2010) Distribution coefficients of 60 elements on TODGA resin: application to Ca, Lu, Hf, U and Th isotope geochemistry. Talanta, in press. doi:10.1016/j.talanta.2010.01.008.

Richter F. M., Davis A. M., Ebel D. S. and Hashimoto A. (2002) Elemental and isotopic fractionation of type B calcium-, aluminum-rich inclusions: experiments, theoretical considerations, and constraints on their thermal evolution. *Geochim. Cosmochim. Acta* **66**(3), 521–540.

Richter F. M., Watson E. B., Mendybaev R. A., Teng F.-Z. and Janney P. E. (2008) Magnesium isotope fractionation in silicate melts by chemical and thermal diffusion. *Geochim. Cosmochim. Acta* **72**, 206–220.

Ringwood A. E. (1989) Significance of the terrestrial Mg/Si ratio. *Earth Planet. Sci. Lett.* **95**, 1–7.

Roden M. F., Trull T., Hart S. R. and Frey F. A. (1994) New He, Nd, Pb, and Sr isotopic constraints on the constitution of the Hawaiian plume: results from Koolau Volcano, Oahu, Hawaii, USA. *Geochim. Cosmochim. Acta* **58**(5), 1431–1440.

Rudnick R. L., McDonough W. F. and Chappell B. W. (1993) Carbonatite metasomatism in the Northern Tanzanian mantle – petrographic and geochemical characteristics. *Earth Planet. Sci. Lett.* **114**(4), 463–475.

Rudnick R. L., McDonough W. F., and Orpin A. (1994) Northern Tanzanian peridotite xenoliths: a comparison with Kaapvaal peridotites and inferences on metasomatic interactions. In *Kimberlites, Related Rocks and Mantle Xenoliths. Proceedings of the 5th International Kimberlite Conference* (eds. H. O. A. Meyer and O. Leonardos), pp. 336–353.

Salters V. J. M., Blichert J., Fekiacova Z., Sachi-Kocher A. and Bizimis M. (2006) Isotope and trace element evidence for depleted lithosphere in the source of enriched Koolau basalts. *Contrib. Mineral. Petrol.* **151**, 297–312.

Schoenberg R. and von Blanckenburg F. (2006) Modes of planetary-scale Fe isotope fractionation. *Earth Planet. Sci. Lett.* **252**(3–4), 342–359.

Scott E. R. D. and Krot A. N. (2003) Chondrites and their components. In *Meteorites, Comets and Planets. Treatise on Geochemistry* (ed. A. M. Davis). Elsevier-Pergamon, Oxford, pp. 143–200.

Seitz H. M. et al. (2007) Lithium isotope composition of ordinary and carbonaceous chondrites, and differentiated planetary bodies: bulk solar system and solar reservoirs. *Earth Planet. Sci. Lett.* **260**, 582–596.

Teng F.-Z., Dauphas N. and Helz R. T. (2008) Iron isotope fractionation during magmatic differentiation in Kilauea Iki lava lake. *Science* **320**, 1620–1622.

Teng F.-Z., Wadhwa M. and Helz R. T. (2007) Investigation of magnesium isotope fractionation during basalt differentiation: implications for a chondritic composition of the terrestrial mantle. *Earth Planet. Sci. Lett.* **261**(1–2), 84–92.

Valbracht P. J., Staudigel H., Honda M., McDougall I. and Davies G. R. (1996) Isotopic tracing of volcanic source regions from Hawaii: decoupling of gaseous from lithophile magma components. *Earth Planet. Sci. Lett.* **144**, 185–198.

Wasson J. T. and Kallemeyn G. W. (1988) Compositions of chondrites. *Philos. Trans. R. Soc. Lond. A* **325**, 535–544.

Wiechert U. and Halliday A. N. (2007) Non-chondritic magnesium and the origins of the inner terrestrial planets. *Earth Planet. Sci. Lett.* **256**, 360–371.

Woodhead J. D., Greenwood P., Harmon R. S. and Stoffers P. (1993) Oxygen isotope evidence for recycled crust in the source of EM-type ocean island basalts. *Nature* **362**, 809–813.

Wu F.-Y., Walker R. J., Yang Y.-H., Yuan H.-L. and Yang J.-H. (2006) The chemical–temporal evolution of lithospheric mantle underlying the North China Craton. *Geochim. Cosmochim. Acta* **70**, 5013–5034.

Yang W., Teng F.-Z. and Zhang H.-F. (2009) Chondritic magnesium isotopic composition of the terrestrial mantle: a case study of peridotite xenoliths from the North China craton. *Earth Planet. Sci. Lett.* **288**(3–4), 475–482. doi:10.1016/j.epsl.2009.10.009.

Young E. D. and Galy A. (2004) The isotope geochemistry and cosmochemistry of magnesium. In *Geochemistry of Non-Traditional Stable Isotopes. Reviews in Mineralogy & Geochem-*

(eds. C. M. Johnson, B. L. Beard and F. Albarede). Mineralogical Society of America, Washington, DC, pp. 197–230.

Young E. D., Tonui E., Manning C. E., Schauble E. A. and Macris C. (2009) Spinel-olivine magnesium isotope thermometry in the mantle and implications for the Mg isotopic composition of Earth. *Earth Planet. Sci. Lett.* **288**, 524–533.

Associate editor: Richard J. Walker